Optimal Sensor Pairing for TDOA based Source Localization and Tracking in Sensor Networks

Wei Meng†, Lihua Xie†, Wendong Xiao‡
† EXQUISITUS, Centre for E-City, School of EEE, Nanyang Technological University, Singapore
‡ School of Automation and Electrical Engineering, University of Science and Technology Beijing, China

***Abstract*—Source localization based on time-difference-of-arrival (TDOA) measurements from spatially separated sensors is an important problem in sensor networks. While extensive research has been performed on algorithm development, limited attention has been paid to sensor geometry design. In this paper, we study the optimal sensor pair geometry for the TDOA based source localization problem. Analytic solutions to the optimal sensor pair geometries, for both static and movable source cases, are derived when there exist no communication constraints. Furthermore, in many applications, sensor platforms such as unmanned aerial vehicles (UAVs) and unmanned ground vehicles (UGVs) are movable, and their movements and the communications between sensors are constrained. The problem becomes how to optimize the trajectories for the moving platforms such that optimal source localization and tracking can be achieved. We extend our work to optimal sensor path planning and cast it as a constrained nonlinear optimization problem. The sequential quadratic programming (SQP) method is adopted for a solution. Computer simulations demonstrate good localization performance.**

***Index Terms*—Wireless sensor network (WSN), source localization, time-difference-of-arrival (TDOA), sensor placement, Fisher information matrix, Cramer-Rao bound (CRB).**

I. Introduction

Source localization using measurements from spatially separated sensors is an important application of wireless sensor networks (WSNs) [1]–[3]. Among various methods for source localization, the time-difference-of-arrival (TDOA) based method is popular and has wide applications. The TDOA based method usually proceeds in a two-step fashion. Firstly, TDOA measurements between sensor pairs are extracted by using a generalized cross correlation (GCC) method [4]. Then in the second step, the estimated TDOA information will be utilized for location estimation.

In this paper, we consider a centralized sensor pairing strategy, where a common reference sensor is used to collect the signals from other nodes and extract the corresponding TDOA measurements. The centralized sensor pairing has a long history of more than 50 years and it is widely used in aerospace systems [5], [6].

It is well known that relative sensor-source geometry plays a significant role in the performance of any particular localization algorithm [7]. The sensor-source geometry characterized by the Cramer-Rao bound (CRB) has been explored in [7]–[13]. Most of the works deal with the static estimation problem where the source is static and its location is fixed. However, few work considers the sensor placement problem when the source location is uncertain. Martinez et al. [9] study the source localization and tracking problem using range-only sensors under an optimal sensor geometry. But they do not take the uncertainty of the source location into account when deriving the optimal sensor placement. In our approach, we study the optimal TDOA sensor pair geometry for both static and movable sources. The trace of the CRB and posterior error covariance are respectively utilized as objective functions to assess the optimality of the relative sensor-source geometry. The prior source location information in the movable source case will also affect the optimal sensor platform formations.

In many applications, we deal with a network of moving sensor platforms such as unmanned aerial vehicles (UAVs). Due to the constraints in communications and control of UAVs, the problem becomes a constrained sensor trajectory optimization for optimal source localization. In this paper, we extend our work to the real-time TDOA sensor trajectory optimization problem. In the literature, the problem of UAV trajectory optimization has been extensively studied, especially for the bearing-only and vision based target tracking problems [12], [14]–[16]. In [15], a network of UAVs is used for a radio source localization using signal strength measurements, where aircraft motion is coordinated through iterative consensus by individual receding horizon controllers on each vehicle. In [16], authors present a cooperative vision-based estimation and tracking system. In [14], the determinant of Fisher information matrix (FIM) is adopted as an objective function for bearing-only sensor trajectory optimization. However, there is little work on TDOA-based sensor trajectory design. In this paper, we cast the TDOA sensor trajectory optimization as a constrained nonlinear optimization problem where constraints in sensor motion and communications are considered. A sequential quadratic programming (SQP) method is adopted as a solution. Computer simulations demonstrate good localization performance.

II. Problem Formulation

We consider a team of M sensor nodes performing source localization and tracking task. Each sensor pair can estimate the time difference of arrival (TDOA) between them by using a generalized cross correlation method (GCC) [4]. The TDOA estimate by the sensor pair $\{i, j\}$ can be written as:

$$\hat{t}_{ij} = \frac{d_{ij}}{v} + e_{ij}, \tag{1}$$

where $d_{ij} = \|\mathbf{x}_i - \theta\| - \|\mathbf{x}_j - \theta\|$, $\mathbf{x}_i = [x_i, y_i]^T$ denotes the coordinates of sensor i, $\theta = [\theta_x, \theta_y]^T$ is the source's coordinates; v denotes the propagation speed of signal; $e_{ij} \sim (0, \sigma^2), \forall 1 \le i, j \le M, i \ne j$, denote the TDOA estimation errors.

The cross covariance of $\hat{t}_{ij}$ and $\hat{t}_{kl}$ denoted by $\mathrm{cov}(\hat{t}_{ij}, \hat{t}_{kl})$ is [6]

$$cov(\hat{t}_{ij}, \hat{t}_{kl}) = \begin{cases} \frac{1}{2}\sigma^2, & i = k \text{ and } j \ne l \text{ or } i \ne k \text{ and } j = l \\ -\frac{1}{2}\sigma^2, & i = l \text{ and } j \ne k \text{ or } i \ne l \text{ and } j = k \\ 0, & \texttt{otherwise}. \end{cases} \tag{2}$$

For M sensors, there are a total number of $M(M-1)/2$ possible sensor pairs and thus $M(M-1)/2$ TDOA measurements. Let

$$\mathcal{I} = \{\{i, j\} | 1 \le i < j \le M\} \tag{3}$$

denote the set of all sensor pairs. $\mathcal{I}'$ is a subset of $\mathcal{I}$ and contains K ($K \le \frac{M(M-1)}{2}$) sensor pairs whose TDOA measurements are used for source localization. By introducing the $K \times 1$ vectors

$$\hat{t} = \begin{bmatrix} \hat{t}_{ij} \\ \vdots \end{bmatrix}_{\{i,j\} \in \mathcal{I}'}, d = \begin{bmatrix} d_{ij} \\ \vdots \end{bmatrix}_{\{i,j\} \in \mathcal{I}'}, e = \begin{bmatrix} e_{ij} \\ \vdots \end{bmatrix}_{\{i,j\} \in \mathcal{I}'}, \tag{4}$$

the measurement model in vector form becomes

$$\hat{t} = \frac{1}{v} d + e. \tag{5}$$

The problem of source localization is to estimate the source location θ given $\hat{t}, \mathbf{x}_i, i = 1, \ldots, M$. In this paper, we will not deal with the algorithm development for source localization and tracking which has been well studied in the literature. Instead, we mainly focus on how to design the optimal sensor pair geometry to improve the source localization and tracking accuracy.

III. Optimal Sensor Pair Geometry without Communication Constraints

In this section, we give a theoretic analysis of optimal sensor pair geometry for the best source localization performance without considering communication constraints. Analytic solutions are derived for both the static and movable source cases.

Most of the existing TDOA based source localization approaches adopt a centralized sensor pairing method to extract the TDOAs in which there is one common reference node to compute TDOA measurements via the generalized cross correlation (GCC) method.

A. Static source scenario

In the static scenario, the localization can be done by using estimation methods such as maximum likelihood method (MLE), nonlinear least-squares (NLS) method, etc.. The localization performance can be explicitly characterized by certain measures, for example, by the Crame-Rao bound (CRB). It is well known that MLE can achieve CRB asymptotically [7]. CRB is related to the sensor-source geometry which gives the lowest bound for error covariance matrix among any unbiased estimators. For an unbiased estimate $\hat{\theta}$ of θ, we find

$$\mathbb{E}[(\hat{\theta} - \theta)(\hat{\theta} - \theta)^T] \ge \mathbf{J}^{-1} = \mathbf{CRB}, \tag{6}$$

where $\mathbf{J}$ is the Fisher information matrix (FIM). The (i, j)th element of $\mathbf{J}$ is given by

$$\mathbf{J}_{i,j}(\theta) = \mathbb{E}\Big[\frac{\partial}{\partial \theta_i} \ln(f(\hat{t}; \theta)) \frac{\partial}{\partial \theta_j} \ln(f(\hat{t}; \theta))\Big],$$

where $f(\hat{t}; \theta)$ is the probability density function (PDF) of $\hat{t}$ given by

$$f(\hat{t}; \theta) = \frac{1}{(2\pi)^{N/2}\sqrt{det(\Sigma)}} \exp\Big[-\frac{1}{2}(\hat{t} - \frac{1}{v}d)^T \Sigma^{-1} (\hat{t} - \frac{1}{v}d)\Big] \tag{7}$$

with Σ the covariance matrix of TDOA error e.

The CRB for TDOA based localization has been derived in [6] which is given by

$$\mathbf{J}^{-1} = v^2 (\mathbf{G} \Sigma^{-1} \mathbf{G}^T)^{-1}, \tag{8}$$

where

$$\mathbf{G} = [g_{ij}, \ldots]_{\{i,j\} \in \mathcal{I}},$$
$$g_{ij} = g_i - g_j,$$
$$g_i = \begin{bmatrix} \frac{\theta_x - x_i}{\sqrt{(\theta_x - x_i)^2 + (\theta_y - y_i)^2}} \\ \frac{\theta_y - y_i}{\sqrt{(\theta_x - x_i)^2 + (\theta_y - y_i)^2}} \end{bmatrix} = \begin{bmatrix} \cos\alpha_i \\ \sin\alpha_i \end{bmatrix}.$$

where α_i denotes the angle of arrival measurement of the ith sensor.

We are interested in the best sensor pair geometry for localization. In this paper, we use a scalar function, the trace of CRB as the objective function to assess the optimality of the relative sensor-source geometry, i.e., A-optimality is considered. For the centralized sensor pairing, without loss of generality, we assign the first sensor as the reference node and define $\mathcal{I}_0$ as the corresponding subset of sensor pairs, i.e., $\mathcal{I}_0 = [\{21\}, \{31\}, \ldots, \{M, 1\}]$. Hence, the TDOA parameter vectors become,

$$\mathbf{G} = [g_{21}, g_{31}, \ldots, g_{M1}]$$
$$\Sigma = 0.5\sigma^2(\mathbf{I} + \mathbf{1}\mathbf{1}^T).$$

The optimal sensor pair geometry for the centralized sensor pairing is summarized in the following theorem.

Theorem 1: Given the set of the sensor pairs $\mathcal{I}_0$, then

$$Tr(\mathbf{J}^{-1}) \ge \frac{4}{bM^2},$$

where $M \ge 3$ denotes the number of the sensors, and $b = \frac{1}{(v\sigma)^2}$. $Tr(\cdot)$ denotes the trace of a matrix and $\mathbf{J}$ is the FIM.

The equality holds if and only if

$$\sum_{i=1}^{M} \cos\alpha_i = 0, \quad \sum_{i=1}^{M} \sin\alpha_i = 0$$
$$\sum_{i=1}^{M} \cos 2\alpha_i = 0, \quad \sum_{i=1}^{M} \sin 2\alpha_i = 0,$$

where α_i denotes the angle of arrival measurement of the ith sensor which is computed with respect to the unbiased estimate $\hat{\theta}$.

Remark 1: From the results of Theorem 1, we can see that the optimal sensor pair geometry does not depend on the ranges between the source and sensors. It only depends on the directions from the source to sensors. This is mainly because that we assume that e_{ij} is distance-independent. Furthermore, in the optimal sensor-source geometry setting, any sensor can be chosen as the reference which results in the same lower bound of the localization performance.

It is well known that a uniform angular array (UAA) is a special case of the above optimal sensor placement strategy, where

$$\alpha_i = \frac{2\pi}{M}(i-1) + \phi, i = 1, 2, \ldots, M, \tag{9}$$

where $\phi \in (0, 2\pi)$ is any given constant. In Fig. 1, we give an example of the three sensor case, where black star and dots denote the source and sensors respectively.

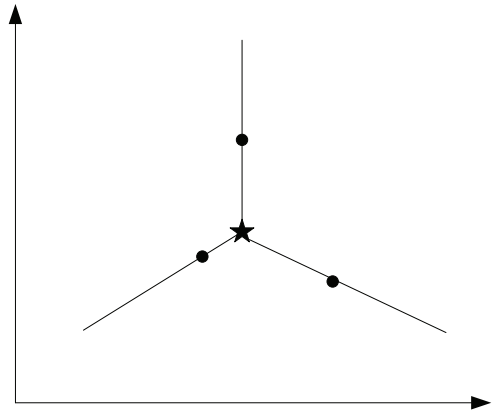

Fig. 1. Optimal three sensor geometry for centralized sensor pairing for static source case (Star and black dots denote the source and sensor location respectively).

B. Movable source case

A movable source can be thought of as a random parameter evolving under a stochastic difference equation [9]. Let $\theta(k)$ denote the source location at time k which evolves according to the following state equation:

$$\theta(k+1) = F_k(\theta(k)) + w(k), \tag{10}$$

for some functions $F_k : \mathbb{R}^2 \to \mathbb{R}^2$, where $\theta(k) = [\theta_x(k), \theta_y(k)]^T$ denotes the source location at time k, $w(k) \sim (0, \Lambda_k)$ is the process noise.

Similarly as before, the TDOA measurement model is given by

$$\hat{t}_{ij}(k) = \frac{d_{ij}}{v}(k) + e_{ij}(k). \tag{11}$$

Extended Kalman filter (EKF) is widely employed for source localization and tracking problem for nonlinear systems. The EKF provides a state estimate $\hat{\theta}(k+1)$ together with an estimate of the covariance of the estimation error, $\mathbf{P}_{k+1|k+1}$, which can be written as [17]:

$$\mathbf{P}_{k+1|k+1} = \left((\mathbf{P}_{k+1|k})^{-1} + \mathbf{J}_{k+1}\right)^{-1}, \tag{12}$$

where $\mathbf{P}_{k+1|k}$ is the one-step prediction error covariance of $\theta(k+1)$ and $\mathbf{J}_{k+1}$ is the Fisher information matrix (FIM) associated with the sensor measurements at time step $k+1$.

Here, we mainly focus on how to design a sensor-source geometry which will enable an optimal localization under certain criterion in terms of the posterior error covariance matrix $\mathbf{P}_{k+1|k}$ (refer to A-optimality/D-optimality/E-optimality). Similar to the static source case, we choose to use the A-optimality criterion. Note that the prior source location information matrix $\mathbf{P}_{k+1|k}$ plays an important role in the geometry design, which has not been investigated in the literature.

Without loss of generality, we focus on a two-dimensional case and assume that

$$\mathbf{P}_{k+1|k} = \begin{bmatrix} p_1 & p_3 \\ p_3 & p_2 \end{bmatrix}, \tag{13}$$

which is positive definite. Then, we define

$$\mathbf{Q}_{k+1} = (\mathbf{P}_{k+1|k+1})^{-1}$$

Combining (12) and (13), $\mathbf{Q}_{k+1}$ can be expressed as in (14), where the subscript, $'k+1'$ is omitted. The detail of the derivation is also omitted here.

Assumption 1: $|\frac{p_1-p_2}{b(p_1p_2-p_3^2)}| \le M$ and $\frac{p_3}{2b(p_1p_2-p_3^2)} \le M$.

For the optimal sensor-source geometry, we have the following result.

Theorem 2: If $\mathcal{I}' = \mathcal{I}_0$, then we have

$$Tr(\mathbf{P}_{k+1|k+1}) \ge \frac{4}{bM + \frac{p_1+p_2}{p_1p_2-p_3^2}}, \tag{15}$$

where M denotes the number of sensors and $M \ge 4$.

Further, under Assumption 1, the equality holds if and only if

C1) $\sum_{i=1}^{M} \cos\alpha_i = 0, \quad \sum_{i=1}^{M} \sin\alpha_i = 0;$

C2) $\sum_{i=1}^{M} \cos 2\alpha_i = \frac{p_1-p_2}{b(p_1p_2-p_3^2)}, \sum_{i=1}^{M} \sin 2\alpha_i = \frac{p_3}{2b(p_1p_2-p_3^2)}.$

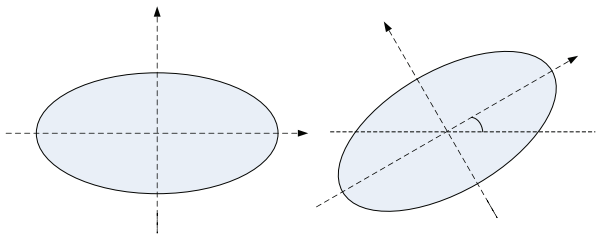

Fig. 2. Effect of p_3

If $|\frac{p_1-p_2}{b(p_1p_2-p_3^2)}| > M$ or $\frac{p_3}{2b(p_1p_2-p_3^2)} > M$, which means that the error correlation between two directions x and y is too high and/or the number of the sensors M is small which can not meet the requirements of the conditions in Theorem 2, we can not force the two eigenvalues of $\mathbf{P}_{k+1|k+1}$ to be equal as we have done in Theorem 2. In this case, it may not be possible

$$\mathbf{Q}=b\begin{bmatrix} \sum_{i=1}^{M}\cos^2\alpha_i-\frac{1}{M}(\sum_{i=1}^{M}\cos\alpha_i)^2+\frac{p_2}{b(p_1p_2-p_3^2)} & \sum_{i=1}^{M}\frac{\sin 2\alpha_i}{2}-\frac{1}{M}\sum_{i=1}^{M}\cos\alpha_i\sum_{i=1}^{M}\sin\alpha_i-\frac{p_3}{b(p_1p_2-p_3^2)} \\ \sum_{i=1}^{M}\frac{\sin 2\alpha_i}{2}-\frac{1}{M}\sum_{i=1}^{M}\cos\alpha_i\sum_{i=1}^{M}\sin\alpha_i-\frac{p_3}{b(p_1p_2-p_3^2)} & \sum_{i=1}^{M}\sin^2\alpha_i-\frac{1}{M}(\sum_{i=1}^{M}\sin\alpha_i)^2+\frac{p_1}{b(p_1p_2-p_3^2)} \end{bmatrix} \tag{14}$$

to get an analytic solution for the sensor-geometry problem, i.e.,

$$\min_{\alpha_i} Tr(\mathbf{P}_{k+1|k+1}) \tag{16}$$

In this case, some numerical algorithms, e.g., gradient search based method, can be used but may only give a local optimal solution.

Comparing the results in Theorem 1 and Theorem 2, we can find that the prior source location information, i.e., $\mathbf{P}_{k+1|k}$, does affect the optimal sensor platform formations for the next time step, i.e., $k+1$. For example, if $p_1 > p_2$, then $\sum_{i=1}^{M}\cos 2\alpha_i > 0$ which is different from that in Theorem 1. However, if $p_1 = p_2$, then $\sum_{i=1}^{M}\cos 2\alpha_i = 0$ which is the same as in Theorem 1. p_3 denotes the error correlation between x and y directions. The value of p_3 will affect the direction of the coordinate system of sensor formation as seen in Fig. 2. Next, we give a simple example to illustrate the conditions in Theorem 2.

Example: Specially, in this example, four sensors will be placed for source localization. Without loss of generality, we choose sensor 1 as the reference node. The source location estimate at time step k is denoted by $\hat{\theta}(k) = [4,4]^T$, and the estimation error covariance matrix $\hat{\mathbf{P}}_{k+1|k}$ is given by

$$\hat{\mathbf{P}}_{k+1|k}=\begin{bmatrix} 10 & 0 \\ 0 & 1 \end{bmatrix} \tag{17}$$

The 1-sigma uncertainty ellipse is plotted in Fig. 3.

The objective is to minimize the mean square error (MSE), i.e., $\min Tr(\mathbf{P}_{k+1|k+1})$. Specially, we assume that $\alpha_i, i = 1,2,3,4$ are $\alpha_1 = \beta, \alpha_2 = -\beta, \alpha_3 = \pi-\beta, \alpha_4 = \pi+\beta$, where $0 \le \beta \le \pi/2$. Then, it can be easily checked that C1 and condition $\sum_{i=1}^{4}\sin 2\alpha_i = 0$ are satisfied. Substituting the α_i into the condition C2, we can obtain

$$4\cos^2\beta = 2+\frac{1}{2b}\Big(1-\frac{1}{10}\Big).$$

Solving the above equation, we can get $\beta = \arccos\sqrt{0.5+\frac{9}{80b}}$. Hence one solution for the optimal sensor placement is presented as follows:

$$\begin{cases} \alpha_1 = \arccos\sqrt{0.5+\frac{9}{80b}} \\ \alpha_2 = 2\pi-\arccos\sqrt{0.5+\frac{9}{80b}} \\ \alpha_3 = \pi-\arccos\sqrt{0.5+\frac{9}{80b}} \\ \alpha_4 = \pi+\arccos\sqrt{0.5+\frac{9}{80b}} \end{cases} \tag{18}$$

The result in (18) is also presented in Fig. 3. Note that the solutions for the above example are not unique.

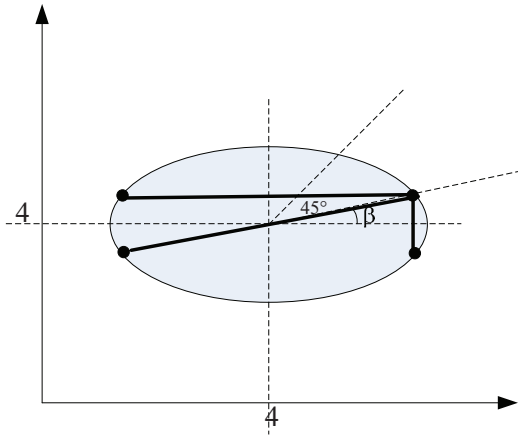

Fig. 3. Optimal three sensor geometry for centralized pairing with source location uncertainty

IV. Optimal Sensor Pair Geometry Optimization with Sensor Motion and Communication Constraints

Until now, we have studied the theoretical characteristics of the optimal sensor pair geometry without considering sensor motion and communication constraints. Although the results for the sensor placement case can provide an intuition about the expected trajectory shape, in real applications, generally, the sensors are not around the sources. In many cases, they are movable and may start from the same place when they take over the source localization and tracking task. Due to the motion constraint of the sensor platforms, such as speed and turning rate of unmanned aerial vehicles (UAVs) and unmanned ground vehicles (UGVs), the optimal geometry obtained above may not be achieved directly. Hence a path planning method is demanded.

In this paper, similarly as before, we consider a 2-dimensional (2D) sensing field. The sensor platform, e.g, unmanned ground vehicle (UGV), is assumed to have a constant velocity and a maximum turn rate constraint. The source of interest is stationary. Note that the method proposed in this paper can be easily extended to the 3D case.

The discrete-time sensor kinematic equations of motion are given by

$$x_i(k+1) = x_i(k) + vT\cos u_i(k), \quad x_i(0) = x_{i_0}, \tag{19}$$

$$y_i(k+1) = y_i(k) + vT\sin u_i(k), \quad y_i(0) = y_{i_0}, \tag{20}$$

where $[x_{i_0}; y_{i_0}]$ is the initial sensor position. $u_i(k)$ denotes the control input (heading angle) for the i-th sensor at time step k. v and T denote the velocity and sampling interval of the sensor platforms respectively.

Since the source is assumed to be stationary, hence the parameters in source motion model (10) are given by $F_k =$

$[1,0;0,1]$ and $\Lambda_k = [0,0;0,0]$. At each step, after sensor takes a measurement, Extended Kalman filter (EKF) is used to update the state estimation, then the sink node will run the sensor pair geometry optimization for the next step. In this paper, the online TDOA sensor pair path planning problem is cast as a constrained nonlinear optimization problem. The objective is to minimize the localization error under the sensor motion and communication constraints, etc. The problem is formulated as follows:

$$\min_{u(k+1)} \mathcal{F}(u(k+1)) = Tr(\mathbf{J}_{k+1}^{-1}) \tag{21}$$

subject to:

$$\|u_i(k+1) - u_i(k)\| \leq u_{max} \tag{22}$$

$$h(\mathbf{x}_i(k+1), \hat{\theta}(k)) \geq r_i \tag{23}$$

$$h(\mathbf{x}_i(k+1), \hat{\theta}(k)) \leq r_i^{'} \tag{24}$$

$$h(\mathbf{x}_i(k+1), \mathbf{x}_j(k+1)) \geq a_{ij} \tag{25}$$

$$h(\mathbf{x}_i(k+1), \mathbf{x}_j(k+1)) \leq b_{ij} \tag{26}$$

where $u(k) = [u_1(k), \ldots, u_M(k)]$. The condition (22) presents the sensor platform input constraint, e.g., UAV turning rate constraint. The inequality (23) is concerned with the sensor to source distance which must be larger than a given threshold where $r_i > 0$. The condition (24) is about the baseline expansion constraint where $r_i^{'}$ is a given constant and $r_i^{'} > r_i$. This is because that in certain situations, minimizing the objective function may result in favoring baseline expansion which is not desired. The condition (25) addresses the collision avoidance between the sensors and a_{ij} is a small constant. Actually, we can also consider the collision avoidance between sensor and potential obstacles. The inequality (26) shows the network connectivity conditions, e.g, sensor communication radius constraints. In this paper, we will not consider the channel noise and packet loss issues, but we assume that sensors can communicate with each other if the distance between them is not larger than a given constant value.

From the problem formulation (Equations (21-26)), we can see that it is a nonlinear optimization problem with both linear and nonlinear constraints. Direct gradient method can not be used for this kind of problems. Generally, the sequential quadratic programming (SQP) algorithm can be utilized. For a numerical solution for this kind of SQP problem, the Lagrangian for this problem is developed in [18].

A. Simulation Results

Next, we show some simulation results. Four UAVs will be used to localize a stationary source. The true source location is $\theta = [0;0]$ with initial guess $\hat{\theta}(0) = [-50;-20], P_0 = [50,0;0,50]$; The initial positions of the UAVs are $[-100;-50], [-98;-50], [-96;-50], [-94;-50]$ respectively. The initial heading for UAVs are all equal to $\frac{\pi}{2}$ (North). The other parameters are $u_{max} = 15^o, r_i = 10\mathbb{m}\ \forall i, r_i^{'} = 200\mathbb{m}\ \forall i, a_{ij} = 1\mathbb{m}, b_{ij} = 20\mathbb{m}, v = 30/s, T = 1, \sigma = 1$.

1) Sensor trajectory optimization: As seen the initial parameters defined above, the starting points of the four UAVs are close to each other. Each UAV is supposed to take 20 measurements only.

Firstly, we investigate the sensor pair geometry optimization with only UAV turning rate constraint. Hence the objective function is as in (21) with (22) as the only constraint. The simulation results are presented in Fig. 4. The red curve in Fig. 4(a) is the trajectory of the reference node. From the figure, we can see that two sensors are trying to move away from the reference node to obtain a large angle subtended at the source. This coincides with our analysis in Section III. It is interesting to note that during the first several steps, the UAVs have not obtained much information around the x axes due to the motion constraints. After five time steps, the localization errors in the x and y axes drop sharply when the UAVs encompass the source.

However, there are several problems for the above scenario. The first one is the baseline expansion problem. From Fig. 4(a), we can find that minimizing the localization error may result in favoring baseline expansion, which is not desired. Another issue is about the sensor communication problem. In real applications, sensors need to communicate with the reference node to do the TDOA estimations. However, as shown in Fig. 4(a), two sensors (green and black curves) move far away from the reference node (red curve). In this case, the communications between them may not be guaranteed. Also in some cases, collision between sensors may occur.

Accordingly, we include all constraints in our optimization problem. The simulation results are shown in Fig. 5. Different from the results in Fig. 4(a), the reference sensor has to keep close to other three sensors to ensure the quality of communications. On the contrary, the sensors tend to keep distance to each other to have a large angle subtended at the source. In addition, there is no baseline expansion when UAVs move towards the source. After 20 measurements, localization error almost converges to zero.

V. Conclusion

In this paper, we have provided a characterization of optimal centralized sensor pairing for static and movable source cases. The CRB and posterior error covariance are utilized to asses the optimality of the relative sensor-source geometry respectively for two different cases. In addition, we extended our work to the sensor pair trajectory optimization problem. The sequential quadratic programming (SQP) method was utilized to solve this constrained nonlinear optimization problem. Simulations results showed that the proposed method can handle the sensor pair path planning under the motion constraints and communication constraint, etc. Besides, it has good localization performance.

References

[1] J. C. Chen, K. Yao, and R. E. Hudson, "Source localization and beamforming," *IEEE Signal Processing Magine*, vol. 19, no. 2, pp. 30–39, 2002.

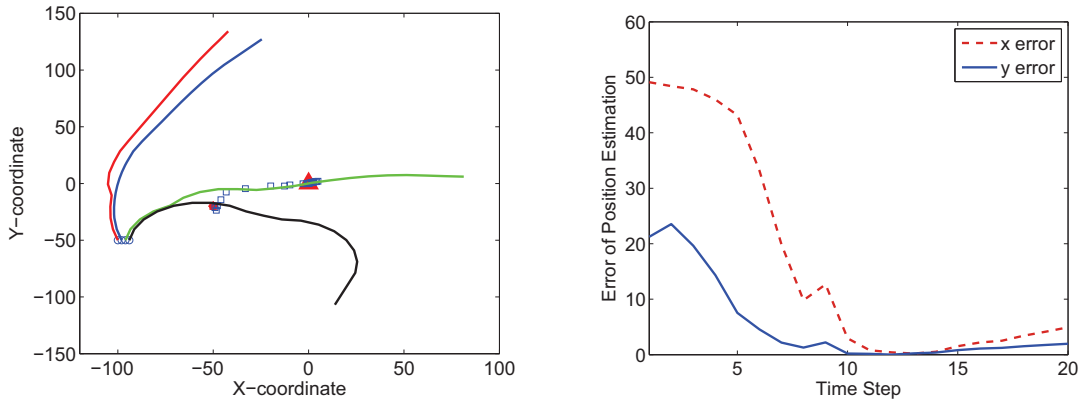

(a) (b)

Fig. 4. Centralized sensor pairing with only turning rate constraints ((a) The triangle and star denote the true target location and the initial guess of the source location. The small rectangle denotes the location estimate at each time step)

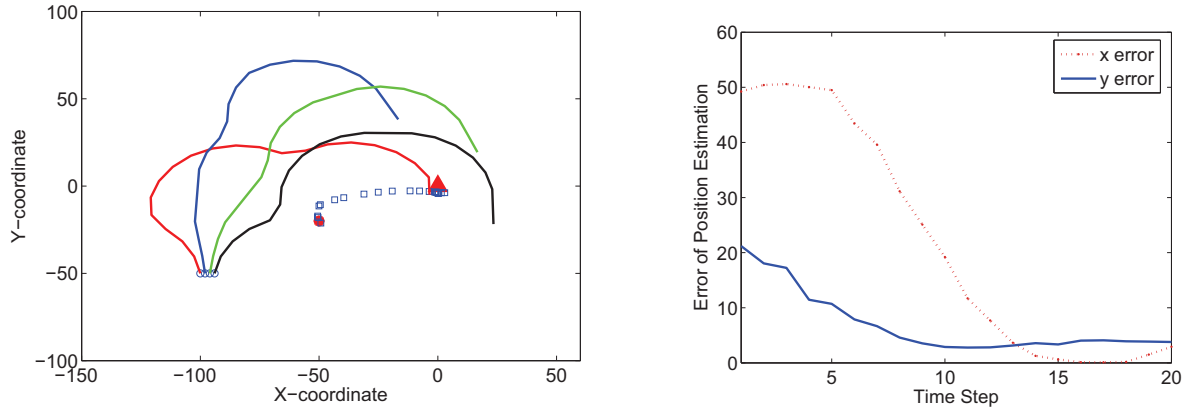

(a) (b)

Fig. 5. Centralized sensor pairing with all constraints ((a) The triangle and star denote the true source location and the initial guess of the source location. The small rectangle denotes the location estimate at each time step)

[2] W. Meng, W. Xiao, and L. Xie, "An efficient EM algorithm for energy-based multisource localization in wireless sensor networks," *IEEE Trans. Instrum. Meas.*, vol. 60, no. 3, pp. 1017–1027, Mar. 2011.

[3] W. Meng, W. Xiao, and L. Xie, "Optimal sensor pairing for TDOA based source localization in sensor networks," *In Proceedings of ICICS*, 13-16, Dec. 2011.

[4] William R. Hahn and Steven A. Tretter, "Optimum processing for delay-vector estimation in passive signal arrays," *IEEE Transactions On Information Theory*, vol. 19, no. 5, pp. 608–614, 1973.

[5] J. Smith and J. Abel, "The spherical interpolation method of source localization," *IEEE Transactions on Oceanic Engineering*, vol. 12, no. 1, pp. 246–252, 1987.

[6] Y. T. Chan and K. C. Ho, "A simple and efficient estimator for hyperbolic location," *IEEE Transactions on Signal Processing*, vol. 42, no. 8, pp. 1905–1915, 1994.

[7] A. N. Bishop, B. Fidan, B. D. O. Anderson, K. Doğancay, and P. N. Pathirana, "Optimality analysis of sensor-target localization geometries," *Automatica*, vol. 46, no. 3, pp. 479–492, 2010.

[8] B. Yang and J. Scheuing, "Cramer-Rao bound and optimum sensor array for source localization from time differences of arrival," *In Proceedings of ICASSP*, 2005.

[9] Sonia Martinez and Francesco Bullo, "Optimal sensor placement and motion coordination for target tracking," *Automatica*, vol. 42, no. 4, pp. 661–668, 2006.

[10] Sanvidha C. K. Herath and Pubudu N. Pathirana, "Optimal sensor separation for AOA based localization via linear sensor array," *In Proceedings of ISSNIP*, 2010.

[11] K. Doğancay and H. Hmam, "Optimal angular sensor separation for AOA localization," *Signal Processing*, vol. 88, no. 5, pp. 1248–1260, 2008.

[12] J.P. Helferty and D.R. Mudgett, "Optimal observer trajectories for bearing only tracking by minimizing the trace of the cramer-rao lower bound," in *Proceedings of the 32nd IEEE Conference on Decision and Control*, Dec 1993.

[13] J. Chen, J. Benesty, and Y. Huang, "Time delay estimation in room acoustic environments: an overview," *EURASIP Journal on Applied Signal Processing*, January 2006.

[14] Y. Oshman and P. Davidson, "Optimization of observer trajectories for bearings-only target localization," *IEEE Transactions on Aerospace and Electronic Systems*, vol. 35, no. 3, pp. 892–902, 1999.

[15] E. Frew, C. Dixon, B. Argrow, and T. Brown, "Radio source localization by a cooperating uav team," in *Proceedings of AIAA Infotech@Aerospace*, September 2005.

[16] B. Bethke, M. Valenti, and J. How, "Cooperative vision based estimation and tracking using multiple uavs," in *Conference of Cooperative Control and Optimization*, January 2007.

[17] Bar-Shalom Y., Li. X., and Kirubarajan T, "Estimation with applications to tracking and navigation," New York: Wiley, 2001.

[18] J. Frederic Bonnans and Jean Charles Gilbert, *Numerical Optimization: Theoretical and Practical Aspects*, Berlin: Springer-Verlag, 2006.